

NATIONAL AERONAUTICS AND SPACE ADMINISTRATION

Ranger IX
Photographs of the Moon

PHOTOGRAPHIC EDITION

JET PROPULSION LABORATORY
CALIFORNIA INSTITUTE OF TECHNOLOGY

December 15, 1965

NATIONAL AERONAUTICS AND SPACE ADMINISTRATION

Ranger IX
Photographs of the Moon

PHOTOGRAPHIC EDITION

JET PROPULSION LABORATORY
CALIFORNIA INSTITUTE OF TECHNOLOGY
December 15, 1965

Jet Propulsion Laboratory
California Institute of Technology

Prepared under Contract No. NAS 7-100
National Aeronautics and Space Administration

Ranger IX Photographs of the Moon



Ranger impact points*

**Lick Observatory photograph*

FOREWORD

This volume of photographs taken by *Ranger IX* is the last in the series of five volumes which present the photographs of the Moon taken by *Ranger VII*, *VIII* and *IX*.^{*} The *Ranger IX* flight concluded the *Ranger* series in a spectacular manner, with the direct broadcast of the B-camera photographs over national television as the spacecraft approached the Moon. *Ranger IX* impacted the Moon on March 24, 1965, within 6 km of the selected target in the crater Alphonsus. The frontispiece shows the impact points of all three successful *Ranger* spacecraft on a telescopic photograph of the Moon, taken with the terminator at 7° East as it was at the time of the *Ranger IX* impact.

Unlike its predecessors, which photographed the relatively simple mare terrain, *Ranger IX* was directed to one of the more complicated areas on the Moon. The impact point selected was slightly northeast of the central peak of Alphonsus. The B camera provided coverage of the rilles and dark-haloed craters near the east wall, while the A camera covered the western side of the crater and the central peak. The coverage of the two cameras thus provided high-resolution photographs of the most interesting features. The area covered by the P cameras was completely overlapped by the A and B cameras, except in the last few frames. The terminal resolution of 30 cm achieved with the P₁ and P₃ cameras exceeded that of both *Ranger VII* and *Ranger VIII*. The last B-camera frame also achieved a resolution of 30 cm, but the transmission of the frame was only about 10% complete at impact.

The selection of photographs for presentation in this volume was based on a careful analysis of the coverage and overlap of the entire set of pictures.^{**} The final choice of 170 frames was made as follows:

1. Seventy of the 220 A-camera frames were selected, with the first 18 at a constant scale increase of about 7.5% between frames and all of the last 52 consecutive frames.

^{*}*Ranger VII, Photographs of the Moon, Part I: Camera "A" Series*, August 27, 1964; *Part II: Camera "B" Series*, December 15, 1964; *Part III: Camera "P" Series*, February 10, 1965; *Ranger VIII, Photographs of the Moon*, December 15, 1965.

^{**}Selection of the photographs was made by E. A. Whitaker of the University of Arizona, the negatives were processed by R. Wichelman of JPL, and the photographic printing was done by Ray Manley, Commercial Photography, Inc., Tucson, Arizona.

2. Thirty-three of the first 165 B frames were chosen with a 4% scale increase between frames, and all of the last 55 frames, for a total of 88 B frames.
3. The last twelve consecutive P frames were selected to present the final high-resolution pictures. The earlier P frames are completely overlapped by the A and B pictures.

This set of volumes is being prepared in order to provide the scientific community with the results of the *Ranger* missions. The efforts of the *Ranger* Experimenter team have led to the publication of the results of the *Ranger VII* mission[†] and will soon be followed by the results of the *Ranger VIII* and *IX* missions.^{††} The *Ranger* Experimenter team which has been conducting the initial scientific evaluation has as its members the following scientists:

<i>Principal Investigator</i>	Dr. Gerard P. Kuiper, Director, Lunar and Planetary Laboratory, University of Arizona, Tucson, Arizona.
<i>Co-experimenters</i>	Mr. R. L. Heacock, Chief, Lunar and Planetary Instruments Section, Jet Propulsion Laboratory, Pasadena, California. Dr. E. M. Shoemaker, Chief, Astrogeology Branch, U.S. Geological Survey, Flagstaff, Arizona. Dr. H. C. Urey, Professor at Large, School of Science and Engineering, University of California at La Jolla, California. Mr. E. A. Whitaker, Research Associate, Lunar and Planetary Laboratory, University of Arizona, Tucson, Arizona.

[†]*Ranger VII, Part II: Experimenters' Analyses and Interpretations*, Technical Report No. 32-700, February 10, 1965.

^{††}*Ranger VIII and IX, Part II: Experimenters' Analyses and Interpretations*, Technical Report No. 32-800 (to be published).

CONTENTS

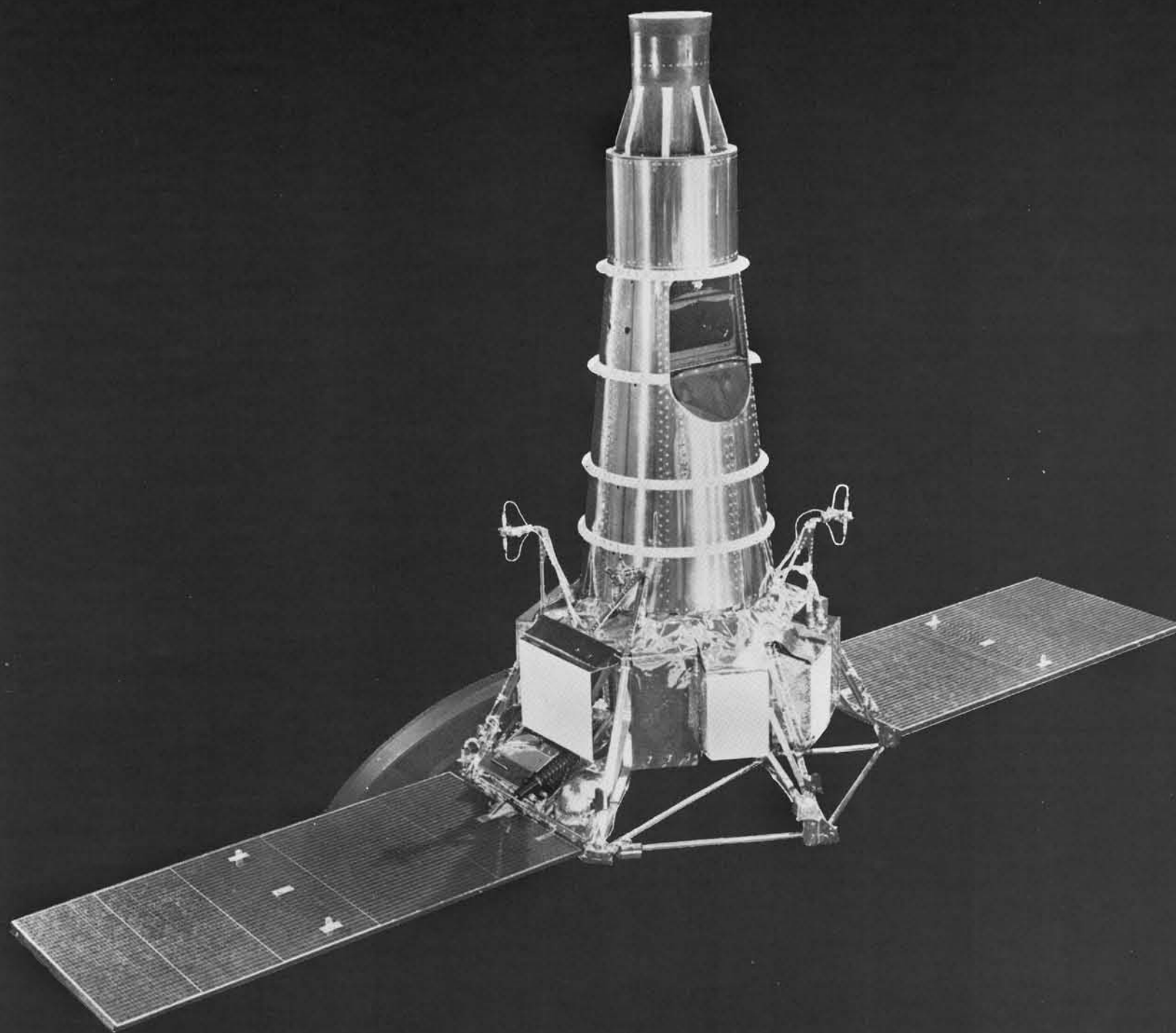
I. Introduction	1
II. <i>Ranger IX</i> Mission Description and Trajectory	2
III. Target Selection and Camera Terminal Alignment	6
IV. Television System Description	7
A. Cameras	7
B. Receiving and Recording Equipment	7
C. Camera Calibration	8
D. Film Processing	9
V. Camera Tables of Values	11
References	17

TABLES

1. Camera characteristics	7
2. <i>Ranger IX</i> preliminary tables of values	13

FIGURES

1. Lunar encounter geometry	3
2. Spacecraft coordinate system	4
3. <i>Ranger IX</i> camera fields of view	5
(a) Cameras A and B	5
(b) Cameras P_1 and P_2	6
(c) Cameras P_3 and P_4	6
4. Typical light-transfer characteristics	8
5. Typical sine-wave response	9
6. <i>Ranger IX</i> area coverage	10
7. Definition of central reticle, deviation north, and scale	11
8. Altitude and range definition	12
9. <i>Ranger IX</i> photometric geometry	12



I. INTRODUCTION*

The development of the basic *Ranger* spacecraft system was initiated in 1959. The spacecraft was conceived as a fully attitude-stabilized platform from which lunar or planetary observations could be made by mounting alternate payloads on top of the basic spacecraft. A new concept involving a parking orbit was also proposed in order to permit maximum payloads to be injected on the most efficient lunar or planetary trajectory. The technique involves two burns of the second stage of the *Atlas/Agena B* launch vehicle to compensate for the nonideal geographical location of the launch pad and provide a more practical daily launch window.

The advantages to be gained from an attitude-stabilized spacecraft configuration include:

1. Maximum effectiveness in generating power by accurately pointing solar panels at the Sun.
2. Establishment of an accurate angle-reference system for use as a coordinate system in which to perform a midcourse maneuver to trim the flight path and as a reference for terminal orientation.
3. Provision of maximum communications by accurately pointing a high-gain antenna at the Earth.
4. Feasibility of using scientific instruments which require direction determination and/or control to make their observations.

The nominal sequence of spacecraft operation after separation from the *Agena B* involves extending the solar panels and pointing the roll axis at the Sun for maximum solar power. The attitude-control system uses inputs from optical sensors to control small cold-gas jets to obtain and maintain proper attitude orientation. When the spacecraft is sufficiently far from the Earth, the antenna hinge angle is nominally set to point the optical Earth sensor and the high-gain antenna at the Earth. The control jets roll the spacecraft until the optical Earth sensor locks onto the Earth and high-gain directional

communication is made possible. Establishing Sun and Earth orientation in this manner provides full attitude stabilization for the cruise mode.

The midcourse maneuver is performed by establishing an appropriate pointing direction relative to the Sun-spacecraft-Earth coordinate system and firing a midcourse rocket engine to obtain the desired velocity increment. A radio-command system transmits the angles and velocity-increment requirements to the spacecraft. The commands are stored and acted upon in a controlled sequence using a gyro-stabilized reference system to achieve the required orientation. Once the midcourse maneuver is complete, the spacecraft automatically resumes the cruise-mode orientation.

The spacecraft has the ability to perform a limited angular orientation in a terminal-maneuver sequence if required. The principal constraint upon orientation geometry involves maintaining the high-gain antenna pointed at the Earth.

The *Ranger* Block III project (consisting of *Ranger VI* through *IX*) was initiated in mid-1961. The objective of high-resolution photographs of the lunar surface could conceptually be achieved through any of several approaches, ranging from systems using long focal-length optics to a technique involving a retro-firing sequence. The approach which was selected used more conventional techniques and available technology. A high-power transmitter was used to provide sufficient video bandwidth for a rapid framing sequence of television pictures to impact. Two separate channels were proposed for redundancy and to permit both narrow- and wide-angle camera coverage.

The camera fields of view were arranged to provide overlapping coverage so that, with a nominal terminal orientation, a nesting sequence of photographs would be obtained from at least one of the wide-angle cameras. The narrow-angle camera frame sequence is over ten times faster than the wide-angle camera sequence to permit operation closer to the surface for higher resolution. The final design of the system included two cameras in the wide-angle system and four cameras in the narrow-angle system.

*The sections that follow were prepared by Gerald M. Smith, Donald E. Willingham, and William E. Kirhofer of the Jet Propulsion Laboratory, California Institute of Technology.

II. RANGER IX MISSION DESCRIPTION AND TRAJECTORY

Ranger IX was launched from Cape Kennedy on March 21, 1965, at 21:37:02 GMT, after a countdown with only 26 min of unscheduled holds. The launch resulted in a trajectory which would intercept the Moon very close to the desired target area on the Moon at impact. A small correction was then calculated, and the midcourse maneuver was executed accordingly. During the launch, all booster-vehicle and spacecraft events occurred as planned. The initial *Atlas D/Agena B* boost placed the *Agena* and spacecraft in a parking orbit over the Atlantic Ocean, where the *Agena* second burn was initiated. Termination of this final boost phase accomplished the injection of the spacecraft into an Earth-Moon transfer orbit. After separation from the *Agena*, the spacecraft solar panels were extended, and Sun and Earth acquisition were accomplished in a normal manner.

Telemetry and doppler velocity data received during the midcourse-motor burn confirmed the desired midcourse correction. The spacecraft then returned to cruise mode by reacquiring the Sun and Earth. Post-midcourse tracking data indicated that the spacecraft would impact the Moon in the selected target area, 13° South and 2.5° West selenocentric coordinates.

After the midcourse maneuver, the terminal approach was analyzed considering the angle of illumination of the lunar surface, the direction of the velocity vector of the spacecraft, and the pointing direction of the camera system. It was established that a terminal orientation maneuver was required to align the camera reference direction along the impact velocity vector. The terminal maneuver sequence was initiated at 12:02:34 GMT and the reorientation of the spacecraft completed by 12:13:59. The wide-angle camera system started taking pictures at 13:49:31 GMT on March 24, 1965, 18 min, 49 sec prior to impact. The narrow-angle system initiated transmission of pictures at 13:49:33 GMT, 18 min, 47 sec prior to impact. Both camera systems operated to impact at 14:08:20 GMT. The last picture was taken 0.25 sec before impact from an altitude of approximately 600 meters. The area read out covers approximately 75×77 meters and has a surface resolution of about 0.3 meters.

The spacecraft encountered the Moon in direct motion along a hyperbolic trajectory, with incoming asymptote direction at an angle

of -5.6° from the lunar equator. The orbit plane was inclined 15.6° to the lunar equator. Thus, the subspacecraft trace on the lunar surface was initially below the lunar equator by approximately 5° and proceeded in a southeasterly direction away from the equator, as shown in Fig. 1.

At the time of the first wide-angle picture, the spacecraft selenocentric south latitude and west longitude were 9.8 and 19.4° , respectively. At impact, the velocity vector was 25.1° from the local vertical in a direction, projected into the local horizon, 99° east of north. The velocity of the spacecraft at impact was 2.671 km/sec. The encounter geometry illustrated in Fig. 1 relates the trajectory and lunar trace with the lunar area viewed by each wide-angle camera.

The *Ranger IX* spacecraft was stabilized by a cold-gas jet attitude-control system. During the cruise mode prior to the terminal maneuver, this system derived its reference from the Sun and Earth. The Sun sensors allowed the spacecraft roll axis to be aligned with the $-Z$ axis toward the Sun. The Earth sensor was used to orient the high-gain antenna toward Earth. This orientation kept the Earth in the Y,Z plane of the spacecraft. The X, Y , and Z orthogonal coordinate system associated with the spacecraft is defined in Fig. 2.

At lunar encounter, the Moon was very near its third quarter, with the projection of the Sun at a selenocentric south latitude and west longitude of 1.5 and 82.2° , respectively. The lunar libration was such that the projection of the Earth was at a lunar north latitude of 1.3° and east longitude of 2.4° . Thus, prior to the terminal maneuver, with the Sun and Earth as reference, the Y,Z spacecraft plane was then inclined to the lunar equator by less than 2° .

In order to align the camera reference direction along the impact velocity vector while keeping the high-gain antenna pointed toward Earth, the terminal maneuver turns performed were an initial pitch turn of 5.2° , a yaw turn of -16.3° , and a second pitch turn of -20.25° . As a result (primarily of the yaw turn), the picture frames were tilted some 20° to the lunar equator.

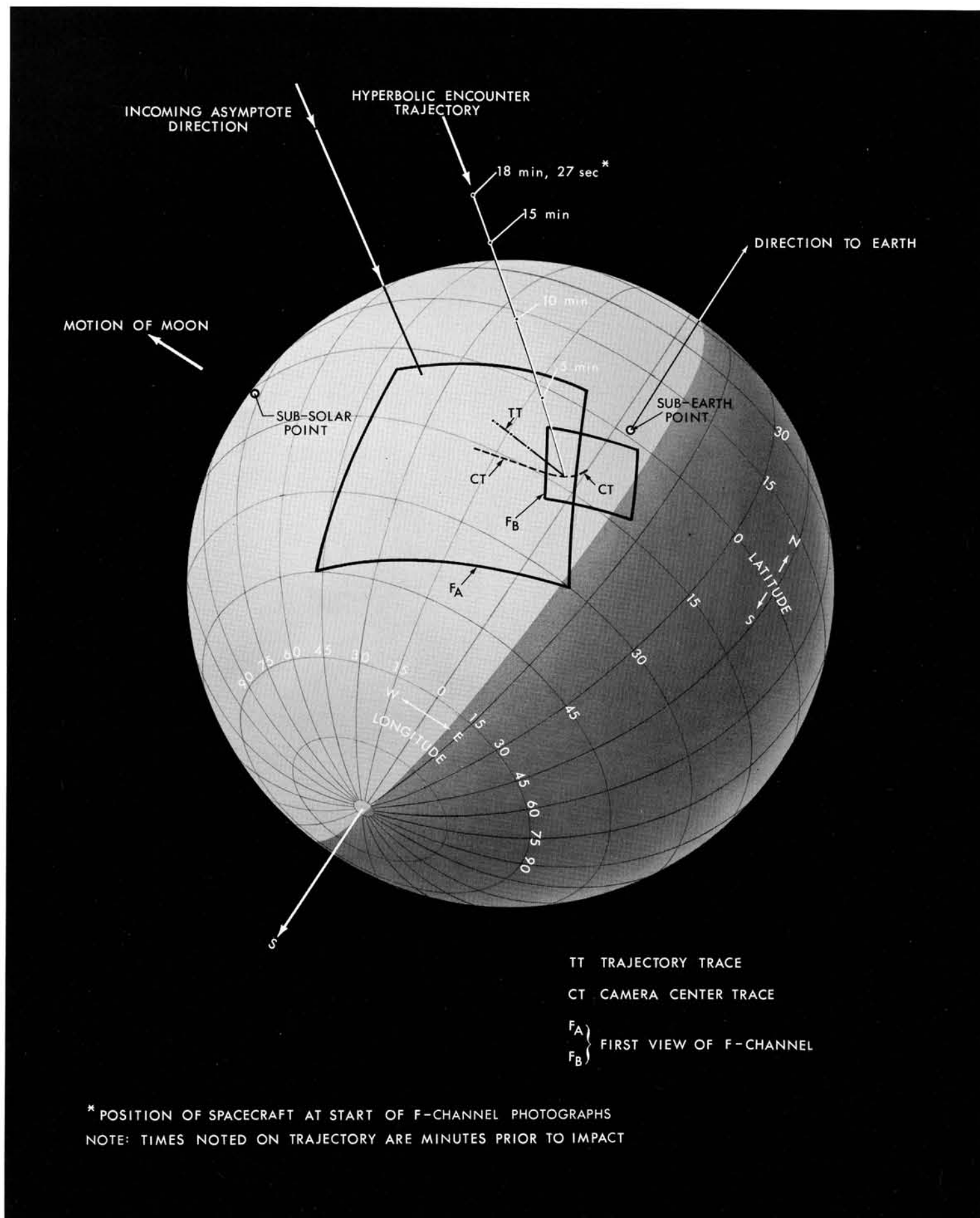


Fig. 1. Lunar encounter geometry



Fig. 2. Spacecraft coordinate system

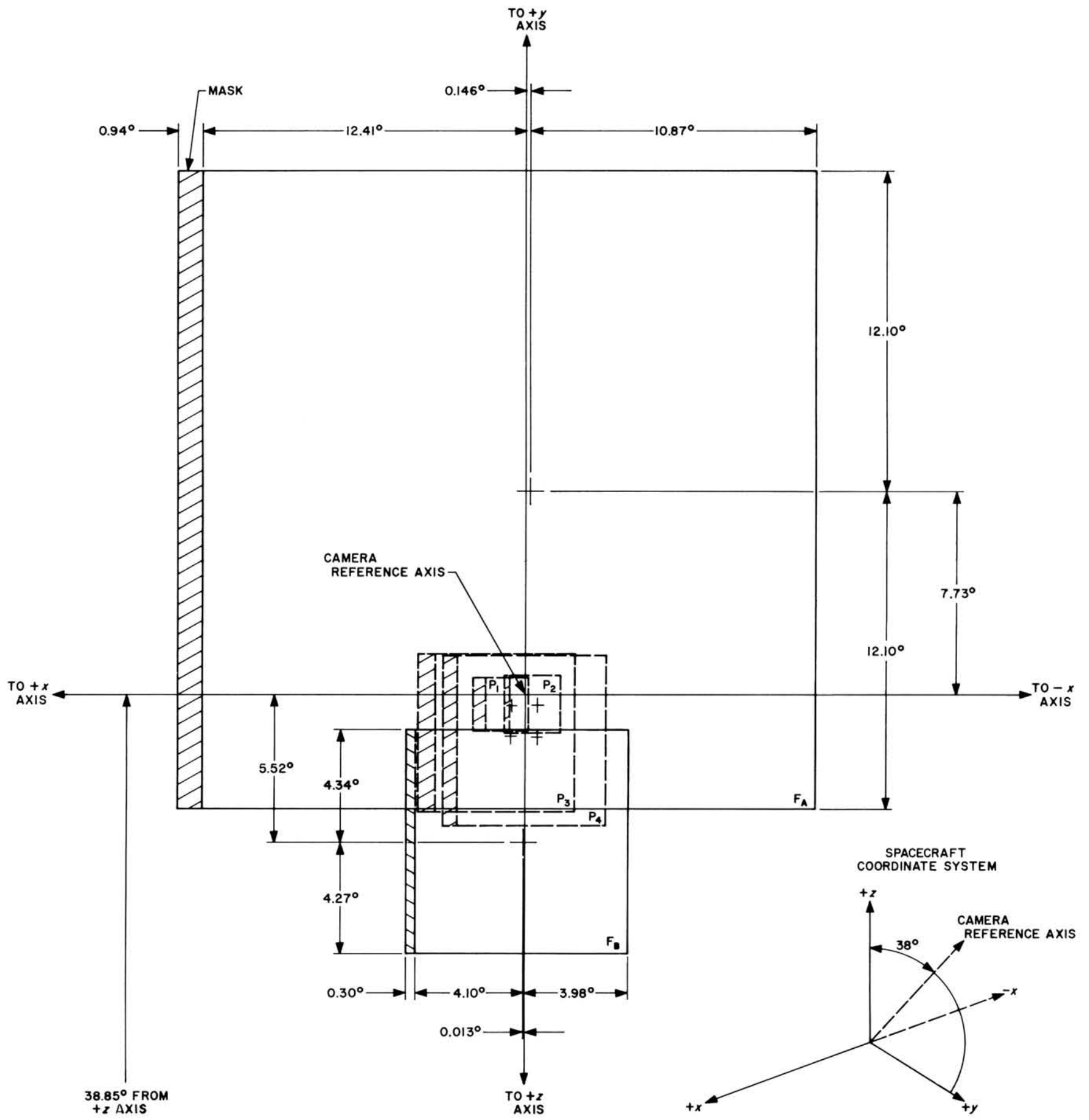


Fig. 3. Ranger IX camera fields of view (a) Cameras A and B

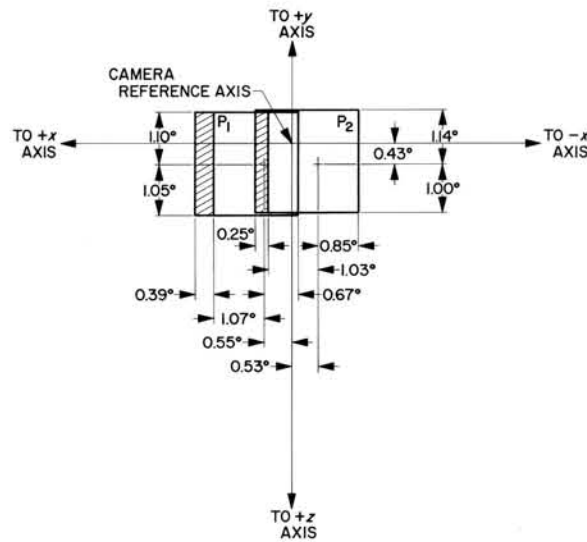
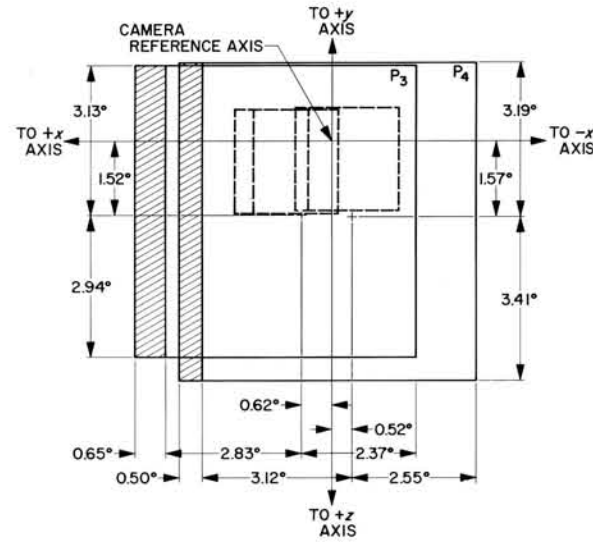
(b) Cameras P_1 and P_2 (c) Cameras P_3 and P_4

Fig. 3. (Cont'd)

III. TARGET SELECTION AND CAMERA TERMINAL ALIGNMENT

The criteria used in selecting *Ranger IX* target areas were somewhat different from those applied to the *Ranger VII* and *Ranger VIII* target selection. The overall objective of characterizing the lunar surface as a whole, rather than specific areas, remained unchanged. *Ranger VII* and *VIII*, however, had successfully provided high-resolution coverage of the two principal types of mare. Because of the similarities found in these areas, it was decided that further coverage of the maria would not be as useful in deriving an overall surface model as would photographs of other terrain types. Of prime interest were highlands and highland basins; the craters Alphonsus and Aristarchus, where unusual activity had been reported; and Copernicus and the region adjacent to it.

During the first 2 days of the launch period, highlands and highland basins were available south of Tranquillitatis; however, these areas were not generally acceptable to the Experimenter team. On the third day, the terminator would be at about 7° East longitude, and the lighting for the crater Alphonsus would be ideal. Because

of the great interest in Alphonsus itself and the several types of highland terrain in and around the crater, it was decided not to use the first 2 days of the launch period. Alphonsus was chosen as the target for the third day, and Aristarchus and Copernicus for subsequent days in the launch period, in case the launch was delayed. The aiming point coordinates for Alphonsus were 2.5° West longitude and 13° South latitude, slightly northeast of the central peak.

In both the *Ranger VII* and *VIII* missions, the cruise-mode orientation of the spacecraft was not altered for the picture-taking sequence. Although the terminal resolution was limited by image motion in each case, the cruise orientation offered other advantages. The situation was somewhat different for *Ranger IX* in that the terminal resolution and area coverage would have been severely limited without adjustment of the camera orientation. The optimum maneuver would be one which aligned the camera axis with the spacecraft velocity vector. Such a maneuver was performed; as a result, the image motion was negligible, and a terminal resolution of about 0.3 meters was achieved.

IV. TELEVISION SYSTEM DESCRIPTION

A. Cameras

The *Ranger* Block III spacecraft television system contains six cameras, divided into two separate channels designated P and F. Each channel is self-contained, with separate power supplies, timers, and transmitters. All six cameras are fundamentally the same, with differences in exposure times, fields of view, lenses, and scan rates distinguishing the individual cameras (Table 1).

Table 1. Camera characteristics

Characteristic	Camera					
	A	B	P ₁	P ₂	P ₃	P ₄
Focal length, mm	25	76	76	76	25	25
f number	1.0	2.0	2.0	2.0	1.0	1.0
Frame time, sec	2.56	2.56	0.2	0.2	0.2	0.2
Horizontal frequency, cps	450	450	1500	1500	1500	1500
Exposure time, msec	5	5	2	2	2	2
Field of view*, deg	25	8.4	2.1	2.1	6.3	6.3
Target size, deg	11	11	2.8	2.8	2.8	2.8
Scan lines	1150	1150	300	300	300	300
Time between frames, sec	5.12	5.12	0.84	0.84	0.84	0.84

* The actual field of view is somewhat smaller than the given numbers because of the presence of a mask at the edge of the vidicon target which is used to determine scene black on each scan of the electron beam.

One-inch-diameter vidicons are used for image sensing. Electromagnetically driven slit-type shutters expose the vidicons. The image is focused on the vidicon target through the shutter, which is placed slightly in front of the focal plane. The vidicon target is made up of a layer of photoconductive material, initially charged by scanning with an electron beam. The image formed on the photoconductive surface causes variations in resistance across the surface which are a function of the image brightness. These variations allow a redistribution of the charge which remains after exposure. In the *Ranger* cameras, the charge pattern formed by the image on the photoconductor remains much longer than in commercial systems, so that the pictures may be taken more slowly. By slowing down the picture-taking rate, it is possible to use a narrow electrical bandwidth, which simplifies the communications problem in transmission of the signal to Earth. After the image has been formed on the photoconductor by operation of the shutter, an electron beam scans the surface and recharges the photoconductor. The variation in charge current is the video signal, which is then amplified several thousand times and sent to the transmitter, where the amplitude variations are converted to frequency variations. The frequency-modulated signal is amplified, and the signals from the two channels are combined and transmitted to Earth through the spacecraft high-gain antenna.

1. F Channel

The F channel has two cameras—the A camera with a 25° field and the B camera with an 8.4° field. Both have 5-msec exposure times;

however, the A camera has a 25-mm f/1.0 lens, while the B camera f/2.0 lens is 76 mm. The combined useful operating range of the two cameras is from about 10 to 1500 ft-L* scene brightness. This large dynamic range allows for the possibility of the spacecraft impacting in a region with poor lighting conditions without appreciable reduction in the quality of the photographs. The electron beam scans an area approximately 11 mm square in 2.5 sec with 1150 lines. The two cameras operate in sequence, so that only one camera is being scanned at a particular time. This allows the signals from the two cameras to be transmitted over a single transmitter. Since each camera requires 2.5 sec to be scanned and then must wait 2.5 sec while the other camera is scanned, there are intervals of about 5 sec between consecutive pictures on a particular camera. During the waiting period, the cameras erase the residual image from the preceding picture and the shutter exposes the vidicon for the next cycle of operation.

2. P Channel

The P channel contains four cameras, designated P₁ through P₄. The same combination of lens types as in the F channel is used in the P cameras. P₁ and P₂ use 76-mm f/2.0 lenses, and P₃ and P₄ use 25-mm f/1.0 lenses, so that the P cameras have the same dynamic range capability as the F cameras. The primary difference between the two sets of cameras is in the scan rates and the portion of the photoconductive target used. The P cameras scan only a 2.8-mm-square segment of the target with 300 scan lines. The time required to scan the area is 0.2 sec. Again, as with the F cameras, only one camera is being scanned at a time, so that all four are coupled into a single transmitter. The time between consecutive pictures on a particular camera is 0.84 sec. Because of the smaller target area of the P cameras, the field of view is correspondingly smaller than that of the F cameras. P₁ and P₂ have approximately 2.1° fields, while the P₃ and P₄ fields are approximately 6.3°. In addition to the differences described above, the P-camera exposure times are shorter than the F exposures. The P shutters are set for a 2-msec exposure to reduce image motion as the spacecraft approaches the lunar surface. The last complete F-camera picture is taken between 2.5 and 5 sec before impact, while the last complete P-camera picture is taken between 0.2 and 0.4 sec because of the faster cycling rate on the P cameras. Image motion is therefore more severe in the last P camera pictures, and shorter exposure times are required. The sequence for one cycle of operation of the P cameras is P₁–P₃–P₂–P₄, so that photographs are taken alternately by a 76-mm lens and a 25-mm lens.

B. Receiving and Recording Equipment

The television signals from the spacecraft are received with 85-ft diameter antennas at two sites, located about 10 mi apart at Goldstone, California. The signals are amplified and mixed by a local oscillator to reduce the signal center frequency to 30 Mc and then sent to the television receiver. Another mixing operation reduces the frequency to 4.5 and 5.5 Mc, respectively, for the two channels. The signal frequency variations are then converted back to amplitude

* 1 ft-L = 1.0764 × 10⁻³ lamberts.

variations in two demodulators (one for each camera channel), whose outputs are the same as the video signals originally generated in the cameras. The video signals are used to control the intensity of an electron beam in a cathode-ray tube, which is scanned in unison with the electron beam in the cameras. The cathode-ray tube reconstructs the original image, which is then photographed on 35-mm film. These recording devices are similar to the commercial kinescopes used for recording television programs on film. Again, there is one recording device for each camera channel, so that two pictures are being recorded at any instant in time, one F camera and one P camera. All the functions discussed above are duplicated at both receiving sites, with one exception. One site utilizes a single film recorder to record the four P cameras, while the other site maintains two film recorders and records both camera channels.

In addition to the film recorders, another means of recording the data is used. The 4.5- and 5.5-Mc signals that go to the demodulators are also sent to another mixer, which reduces the center frequency still further to 500 kc. These signals are recorded on magnetic tape at both sites. Two such recorders are used at each receiving station. In order to obtain film records from the magnetic tapes, they are played through a demodulator, and the video signal is applied to the film recorder as discussed above.

C. Camera Calibration

The calibration of the cameras involves three principal aspects of camera performance: light-transfer characteristic (photometric calibration), sine-wave response (modulation transfer function), and system noise. In addition, data on geometric distortion are obtained.

Subsequent to the *Ranger VII* mission, the f/2-camera video amplifiers were adjusted to increase the video amplification. This

adjustment reduced the peak illumination which could be accepted; however, since both *Ranger VIII* and *IX* were targeted within 15° of the terminator, the expected scene brightness was well within the dynamic range of the cameras. Figure 4 shows a typical light-transfer characteristic with the adjusted amplification. The adjustment provided a slight improvement in signal-to-noise ratio in the received pictures.

1. Light-Transfer Characteristic

In order to obtain some absolute photometric information about the lunar surface, camera sensitivity is measured as a function of scene brightness. Using a set of collimators to simulate the scene, the cameras are exposed to various brightness levels before launch, and the camera signal output is recorded on magnetic tape. The magnetic tape is then played back through the recording equipment at Goldstone, and the calibration data are recorded on the same film as the lunar photographs in order to eliminate errors due to differences in film strips processed at different times. The variation in development of a single strip from one end to the other is negligible. The net result, then, is the functional relationship between film density and collimator brightness. In order to account for the differences between the spectral emission characteristics of the collimators and the reflected solar radiation from the lunar scene, a series of spectral measurements is made on all the instrumentation. A correction factor is then calculated to correct the collimator brightness to lunar scene brightness. Reference 5 describes this procedure. Since the photometric calibration is on the same film as the photographic data, it can be carried through subsequent copying operations. A typical light-transfer characteristic of scene brightness vs. negative film density for a 76-mm and a 25-mm camera is shown in Fig. 4. The accuracy of the photometric calibration is limited primarily by vidicon nonuniformities and variations in exposure times, and is expected to be about $\pm 20\%$.

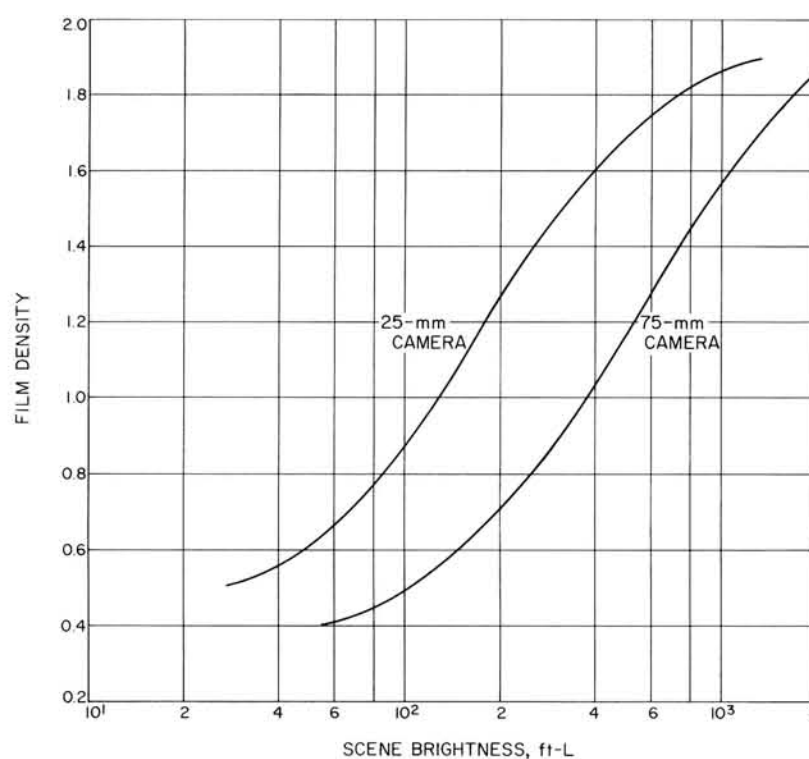


Fig. 4. Typical light-transfer characteristics

2. Sine-Wave Response

In order to obtain the approximate mathematical description of the system required for the figure of merit, it is necessary to determine the sine-wave response of the system. There are a number of ways of obtaining such data. The most direct method is the use of slides with sinusoidal variations in transmission which are then placed in the calibration collimators to illuminate the cameras. A film recording is made, and then the film is scanned with a microphotometer to determine the sine-wave response. A typical response curve is shown in Fig. 5.

3. System Noise and Geometric Distortion

Noise is one of the critical parameters of a photographic system which is required to characterize the system. For a television system, it is convenient to combine film granularity with electrical noise generated in the camera and the communication system to obtain an over-all measure of system noise. The over-all noise is measured by scanning a film recording with a microphotometer. The resulting record is then analyzed to calculate the root-mean-square variations in transmission.

Geometric distortion is determined by inserting a slide in the collimators which has been ruled horizontally and vertically. Photographs of the slide are then used to correct the distortion.

D. Film Processing

The film used in the *Ranger* missions was Eastman Kodak television recording film, type 5374. The negatives were developed by a commercial film processor* to a gamma of 1.4. The photographs in this volume were made using the following procedure:

1. The magnetic tape recorded during the mission was replayed and recorded on film.
2. 8×10 -in. positives of Du Pont Commercial S film were prepared by enlarging the 35-mm negatives, using some manual dodging.
3. The 8×10 -in. positives were contact-printed, and the same film was used to prepare negatives.
4. The photographs were contact-printed from the negatives, with some additional dodging done in the contact printer.

*Consolidated Film Industries, Hollywood, California.

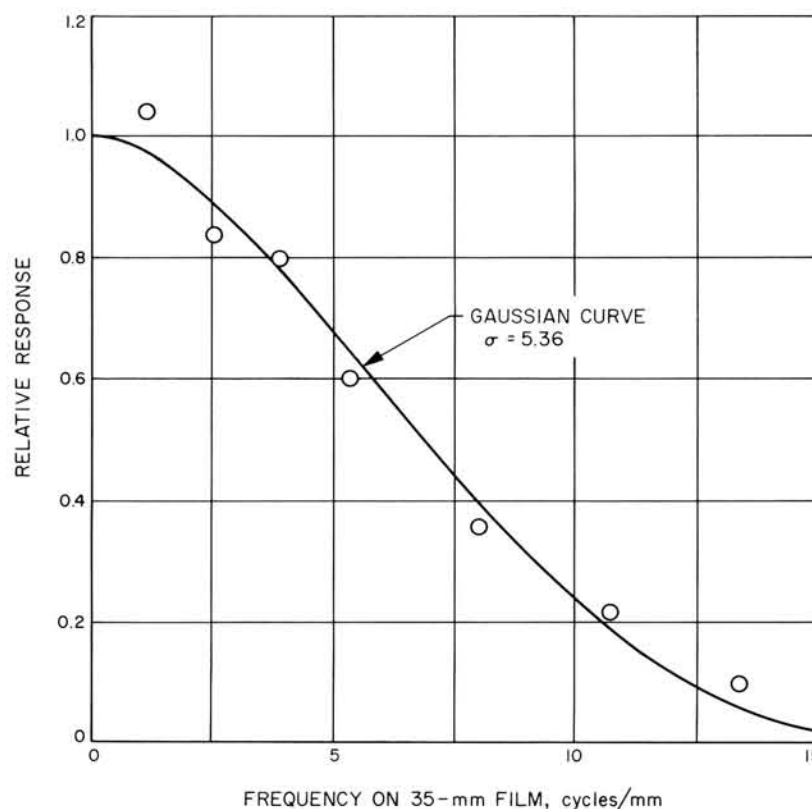


Fig. 5. Typical sine-wave response



Fig. 6. Ranger IX area coverage

V. CAMERA TABLES OF VALUES

The first full-scan A- and B-camera photographs encompass the entire area photographed by *Ranger IX*; this lunar coverage is indicated in Fig. 6.*

Repetition of some permanent camera surface characteristics will be noted in each frame. These irregularities should be ignored in any photograph interpretation studies.

The parameters listed in the preliminary tables of values (Table 2) are defined below:

Spacecraft

Altitude: The distance from the spacecraft to the surface directly below.

Latitude, longitude: The selenocentric position of the point of intersection with the surface of a line connecting the spacecraft and the center of the Moon. This defines the surface point directly below the spacecraft.

*Lick Observatory photograph.

Photograph

Central reticle: The principal cross mark on the camera face (Fig. 7).

Latitude, longitude: The surface point in selenocentric coordinates covered by the central reticle.

Slant range: The distance from the spacecraft to the surface point covered by the central reticle (Fig. 8).

Incidence, phase, emission angles: The emission angle is the angle between the local surface normal and the camera axis. The incidence angle is the angle between the local surface normal and the direction of illumination. The phase angle is measured between the illumination direction and the camera axis. These three angles form the photometric geometry. They can be oriented by noting that the direction of illumination of the observed point is parallel to the line passing through the subsolar point and the Moon center (neglecting parallax) and that the emission angle is measured in the plane formed by the spacecraft surface point and the local normal (Fig. 9). For *Ranger IX*, the subsolar point was at -1.48° latitude and -82.08° longitude.

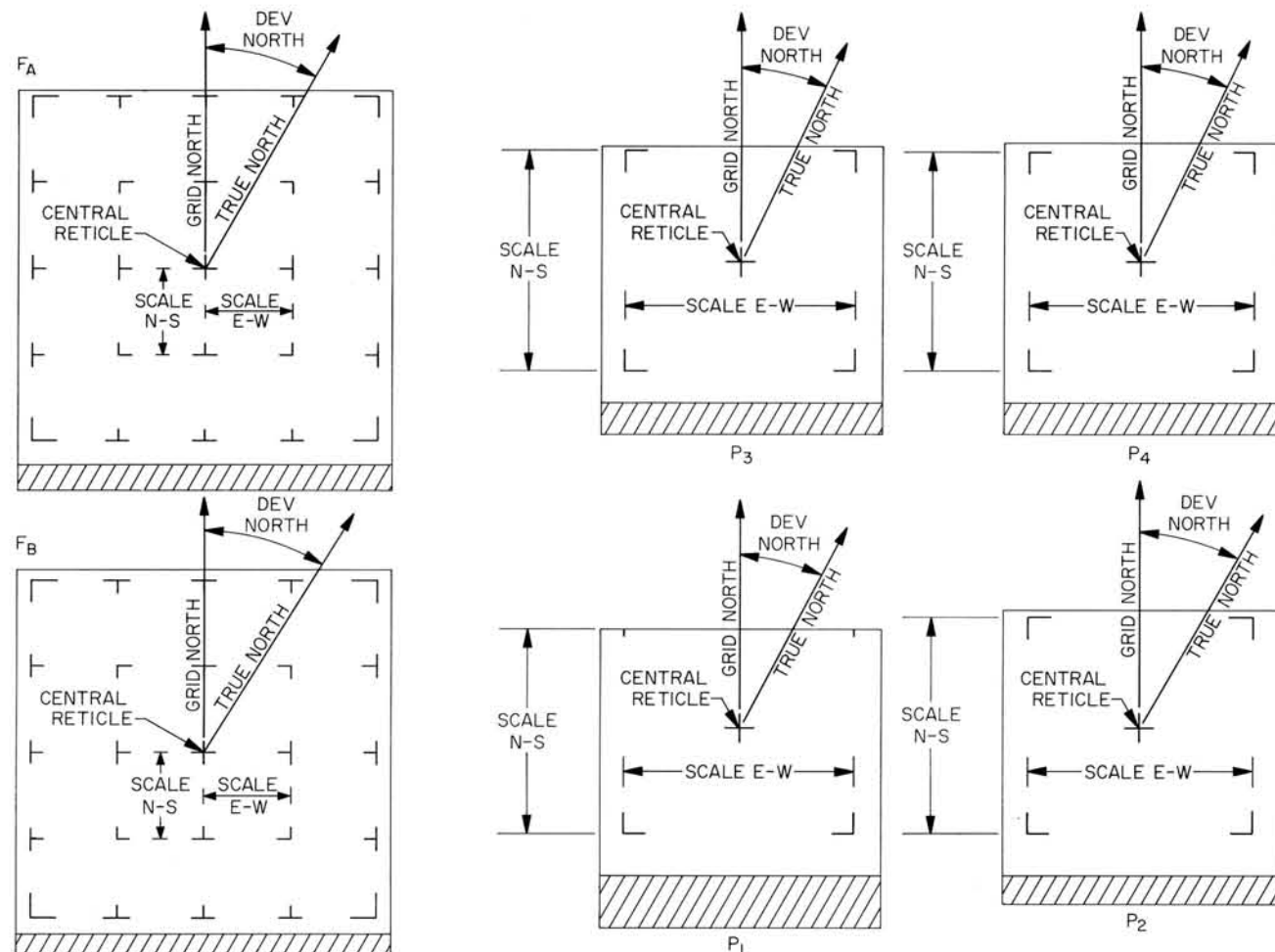


Fig. 7. Definition of central reticle, deviation north, and scale

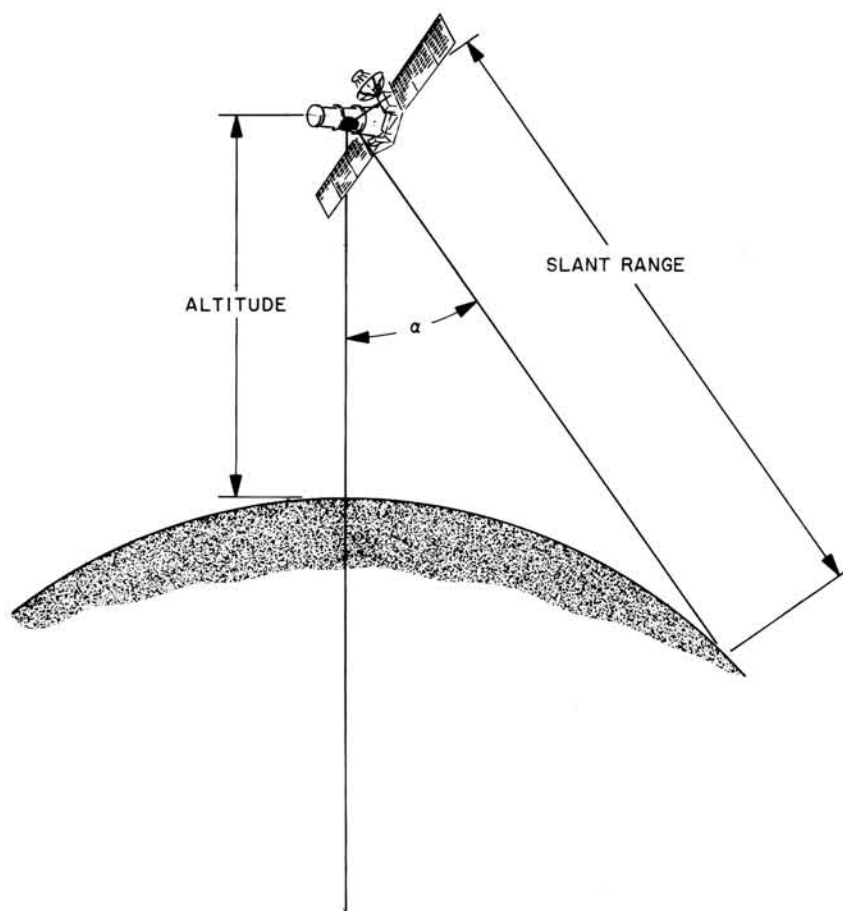


Fig. 8. Altitude and range definition

Scale (E-W, N-S): The distances between the surface points covered by the reticles are indicated in Fig. 7.

Deviation north: Grid north is defined by a straight line drawn from the central reticle to the middle reticle in the north margin of the A- and B-camera photographs. For the

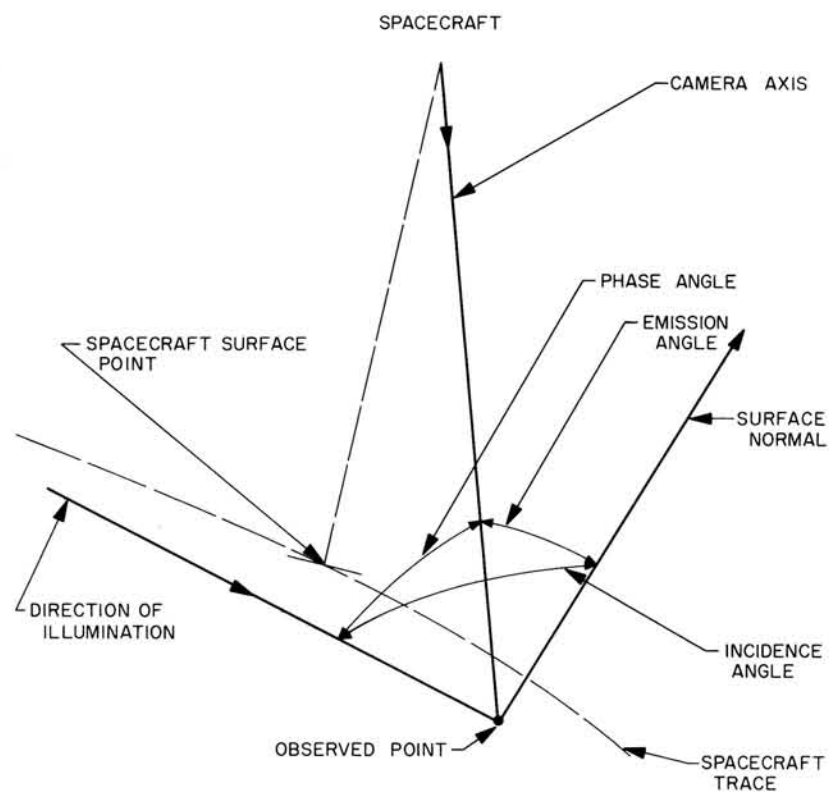


Fig. 9. Ranger IX photometric geometry

P-camera pictures, grid north is defined by a straight line, parallel to the reticle pattern or the edge of the picture, drawn from the central reticle toward the north margin of the photograph. The deviation is the clockwise rotation from grid north to the direction of true north at the central reticle. Convergence of the meridians is appreciable in all but the P_1 - and P_2 -camera photographs, including the larger-scale pictures, and directions at the central reticles cannot be transferred to the left and right margins without introducing errors (Fig. 7).

Table 2. Ranger IX preliminary tables of values
a. Camera A

Photo number	GMT of frame exposure March 24, 1965	Spacecraft			Photograph (central reticle)						Scale, km		Deviation north, deg
		Altitude, km	Latitude, deg	Longitude, deg	Latitude, deg	Longitude, deg	Slant range, km	Incidence angle, deg	Phase angle, deg	Emission angle, deg	E-W	N-S	
1	13:49:40.862	2363.01	-9.75	-19.32	-15.37	-18.68	2377.62	63.8	62.1	9.8	235.76	227.78	17.6
2	13:51:07.902	2195.62	-9.87	-18.73	-15.28	-17.49	2210.09	65.0	62.2	9.9	218.05	211.26	17.9
3	13:52:29.822	2036.31	-10.00	-18.13	-15.23	-16.48	2050.90	66.0	62.5	10.1	201.65	195.73	18.1
4	13:53:51.742	1875.18	-10.14	-17.47	-15.08	-15.16	1890.12	67.2	62.4	10.4	185.01	179.93	18.4
5	13:55:03.422	1732.56	-10.27	-16.84	-14.95	-14.00	1748.12	68.3	62.4	10.8	170.57	166.06	18.7
6	13:56:09.982	1598.69	-10.40	-16.21	-14.84	-13.02	1614.83	69.3	62.4	11.3	157.25	153.15	18.9
7	13:57:11.422	1473.79	-10.53	-15.58	-14.74	-12.09	1490.54	70.2	62.5	11.7	144.93	141.15	19.1
8	13:58:07.742	1358.10	-10.65	-14.95	-14.59	-11.18	1375.51	71.1	62.4	12.2	133.58	130.04	19.4
9	13:58:58.942	1251.89	-10.77	-14.34	-14.46	-10.39	1269.70	71.8	62.4	12.6	123.21	119.87	19.5
10	13:59:45.022	1155.38	-10.89	-13.75	-14.33	-9.69	1173.41	72.5	62.4	13.0	113.82	110.64	19.7
11	14:00:25.982	1068.84	-11.00	-13.19	-14.22	-9.10	1086.92	73.1	62.5	13.3	105.41	102.39	19.8
12	14:01:06.942	981.55	-11.11	-12.59	-14.12	-8.51	999.61	73.6	62.5	13.7	96.94	94.08	19.9
13	14:01:42.782	904.52	-11.21	-12.03	-14.03	-7.96	992.62	74.2	62.5	14.1	89.49	86.75	20.0
14	14:02:13.502	837.99	-11.31	-11.53	-13.95	-7.50	856.00	74.6	62.5	14.4	83.05	80.43	20.2
15	14:02:44.222	770.97	-11.41	-11.00	-13.87	-7.05	788.74	75.1	62.5	14.7	76.55	74.06	20.2
16	14:03:14.942	703.45	-11.51	-10.44	-13.79	-6.60	720.85	75.5	62.5	15.0	69.99	67.64	20.3
17	14:03:35.422	658.14	-11.58	-10.04	-13.73	-6.29	675.28	75.8	62.5	15.2	65.59	63.33	20.4
18	14:03:50.782	624.00	-11.63	-9.74	-13.69	-6.05	640.94	76.0	62.5	15.4	62.28	60.08	20.4
19	14:03:55.902	612.59	-11.65	-9.64	-13.67	-5.97	629.46	76.1	62.5	15.5	61.17	59.00	20.5
20	14:04:01.022	601.17	-11.67	-9.53	-13.66	-5.90	617.95	76.2	62.5	15.6	60.06	57.91	20.5
21	14:04:06.142	589.73	-11.69	-9.43	-13.64	-5.82	606.40	76.3	62.5	15.6	58.95	56.82	20.5
22	14:04:11.262	578.27	-11.71	-9.32	-13.63	-5.74	594.84	76.3	62.5	15.7	57.83	55.73	20.5
23	14:04:16.382	566.80	-11.73	-9.21	-13.62	-5.67	583.25	76.4	62.5	15.7	56.71	54.64	20.5
24	14:04:21.502	555.31	-11.75	-9.10	-13.60	-5.59	571.64	76.5	62.5	15.8	55.59	53.55	20.5
25	14:04:26.622	543.80	-11.76	-8.99	-13.59	-5.52	560.00	76.6	62.5	15.9	54.47	52.45	20.6
26	14:04:31.742	532.28	-11.78	-8.88	-13.57	-5.44	548.34	76.6	62.5	15.9	53.34	51.35	20.6
27	14:04:36.862	520.74	-11.80	-8.77	-13.56	-5.37	536.65	76.7	62.5	16.0	52.21	50.25	20.6
28	14:04:41.982	509.19	-11.82	-8.66	-13.54	-5.30	524.94	76.8	62.5	16.0	51.07	49.15	20.6
29	14:04:47.102	497.62	-11.84	-8.54	-13.53	-5.22	513.20	76.8	62.5	16.1	49.94	48.04	20.6
30	14:04:52.222	486.03	-11.86	-8.43	-13.51	-5.15	501.44	76.9	62.5	16.2	48.80	46.94	20.6
31	14:04:57.342	474.43	-11.88	-8.31	-13.50	-5.08	489.66	77.0	62.5	16.2	47.66	45.83	20.7
32	14:05:02.462	462.81	-11.90	-8.19	-13.48	-5.00	477.85	77.1	62.5	16.3	46.52	44.72	20.7
33	14:05:07.582	451.17	-11.92	-8.07	-13.47	-4.93	466.01	77.1	62.5	16.3	45.37	43.61	20.7
34	14:05:12.702	439.51	-11.95	-7.95	-13.45	-4.86	454.15	77.2	62.5	16.4	44.22	42.49	20.7
35	14:05:17.822	427.84	-11.97	-7.83	-13.44	-4.79	442.26	77.3	62.5	16.4	43.07	41.38	20.7
36	14:05:22.942	416.15	-11.99	-7.71	-13.42	-4.72	430.35	77.3	62.5	16.5	41.92	40.26	20.7
37	14:05:28.062	404.44	-12.01	-7.58	-13.41	-4.65	418.41	77.4	62.5	16.5	40.76	39.14	20.8
38	14:05:33.182	392.72	-12.03	-7.46	-13.39	-4.58	406.44	77.5	62.5	16.6	39.60	38.01	20.8
39	14:05:38.302	380.97	-12.05	-7.33	-13.38	-4.51	394.44	77.5	62.5	16.6	38.43	36.89	20.8
40	14:05:43.422	369.21	-12.07	-7.20	-13.36	-4.44	382.42	77.6	62.5	16.7	37.27	35.76	20.8
41	14:05:48.542	357.43	-12.10	-7.07	-13.35	-4.37	370.37	77.7	62.5	16.7	36.10	34.63	20.8
42	14:05:53.662	345.63	-12.12	-6.94	-13.33	-4.30	358.30	77.8	62.5	16.8	34.93	33.50	20.8
43	14:05:58.782	333.82	-12.14	-6.80	-13.32	-4.23	346.19	77.8	62.5	16.8	33.75	32.36	20.9
44	14:06:03.902	321.98	-12.16	-6.67	-13.30	-4.16	334.07	77.9	62.5	16.9	32.57	31.23	20.9
45	14:06:09.022	310.13	-12.19	-6.53	-13.28	-4.09	321.92	78.0	62.5	16.9	31.40	30.09	20.9
46	14:06:14.142	298.25	-12.21	-6.39	-13.27	-4.02	309.74	78.0	62.5	17.0	30.21	28.95	20.9
47	14:06:19.262	286.36	-12.23	-6.25	-13.25	-3.95	297.53	78.1	62.5	17.0	29.03	27.80	20.9
48	14:06:24.382	274.45	-12.25	-6.11	-13.24	-3.88	285.29	78.2	62.5	17.1	27.84	26.66	20.9
49	14:06:29.502	262.52	-12.28	-5.97	-13.22	-3.81	273.02	78.2	62.5	17.1	26.64	25.51	20.9
50	14:06:34.622	250.57	-12.30	-5.82	-13.21	-3.74	260.73	78.3	62.5	17.2	25.45	24.36	21.0
51	14:06:39.742	238.60	-12.33	-5.67	-13.19	-3.67	248.40	78.4	62.5	17.3	24.25	23.20	21.0
52	14:06:44.862	226.61	-12.35	-5.52	-13.17	-3.60	236.04	78.4	62.5	17.3	23.05	22.05	21.0
53	14:06:49.982	214.60	-12.37	-5.37	-13.16	-3.53	223.65	78.5	62.5	17.4	21.84	20.89	21.0
54	14:06:55.102	202.57	-12.40	-5.22	-13.14	-3.46	211.22	78.6	62.5	17.4	20.63	19.72	21.0
55	14:07:00.222	190.52	-12.42	-5.07	-13.12	-3.39	198.77	78.6	62.5	17.5	19.42	18.56	21.0
56	14:07:05.342	178.45	-12.45	-4.91	-13.11	-3.33	186.28	78.7	62.5	17.5	18.20	17.39	21.1
57	14:07:10.462	166.35	-12.47	-4.75	-13.09	-3.26	173.75	78.8	62.5	17.6	16.98	16.22	21.1
58	14:07:15.582	154.24	-12.50	-4.59	-13.07	-3.19	161.19	78.8	62.5	17.6	15.76	15.05	21.1
59	14:07:20.702	142.11	-12.52	-4.43	-13.05	-3.12	148.59	78.9	62.5	17.7	14.53	13.87	21.1
60	14:07:25.822	129.95	-12.55	-4.26	-13.04	-3.06	135.96	79.0	62.5	17.7	13.30	12.69	21.1
61	14:07:30.942	117.78	-12.58	-4.10	-13.02	-2.99	123.30	79.0	62.5	17.8	12.06	11.51	21.1
62	14:07:36.062	105.58	-12.60	-3.93	-13.00	-2.92	110.59	79.1	62.5	17.9	10.82	10.32	21.1
63	14:07:41.182	93.36	-12.63	-3.75	-12.98	-2.86	97.85	79.2	62.5	17.9	9.57	9.13	21.2
64	14:07:43.302	88.29	-12.64	-3.68	-12.97	-2.83	92.56	79.2	62.5	17.9	9.06	8.64	21.2

Table 2a. (Cont'd)

Photo number	GMT of frame exposure March 24, 1965	Spacecraft			Photograph (central reticle)						Scale, km		Deviation north, deg
		Altitude, km	Latitude, deg	Longitude, deg	Latitude, deg	Longitude, deg	Slant range, km	Incidence angle, deg	Phase angle, deg	Emission angle, deg	E-W	N-S	
65	14:07:51.422	68.85	-12.68	-3.40	-12.95	-2.73	72.26	79.3	62.5	18.0	7.07	6.74	21.2
66	14:07:56.542	56.57	-12.71	-3.22	-12.93	-2.66	59.40	79.4	62.5	18.1	5.82	5.54	21.2
67	14:08:01.662	44.26	-12.74	-3.04	-12.91	-2.60	46.50	79.4	62.5	18.1	4.55	4.34	21.2
68	14:08:06.782	31.93	-12.77	-2.86	-12.89	-2.53	33.57	79.5	62.5	18.2	3.29	3.13	21.2
69	14:08:11.902	19.57	-12.80	-2.67	-12.87	-2.47	20.59	79.5	62.5	18.2	2.02	1.92	21.2
70	14:08:17.022	7.20	-12.82	-2.48	-12.85	-2.41	7.58	79.6	62.5	18.3	0.74	0.71	21.3
IMPACT	14:08:19.994												

Table 2. (Cont'd)
b. Camera B

Photo number	GMT of frame exposure March 24, 1965	Spacecraft			Photograph (central reticle)						Scale, km		Deviation north, deg
		Altitude, km	Latitude, deg	Longitude, deg	Latitude, deg	Longitude, deg	Slant range, km	Incidence angle, deg	Phase angle, deg	Emission angle, deg	E-W	N-S	
1	13:49:43.422	2358.12	-9.75	-19.30	-9.52	0.26	2521.74	82.1	49.6	32.4	97.84	82.55	20.8
2	13:50:29.502	2269.70	-9.82	-19.00	-9.69	0.21	2429.81	82.0	49.7	32.3	94.09	79.59	20.9
3	13:51:10.462	2190.67	-9.88	-18.71	-9.83	0.15	2347.39	81.9	49.7	32.2	90.73	76.91	21.0
4	13:51:51.422	2111.21	-9.94	-18.42	-10.00	0.03	2263.52	81.8	49.8	32.0	87.22	74.21	21.0
5	13:52:32.382	2031.31	-10.01	-18.11	-10.16	-0.09	2179.02	81.7	49.9	31.8	83.70	71.47	21.1
6	13:53:13.342	1950.95	-10.07	-17.79	-10.27	-0.06	2096.55	81.8	49.9	31.8	80.53	68.79	21.1
7	13:53:54.302	1870.11	-10.14	-17.45	-10.39	0.02	2014.08	81.8	49.9	31.9	77.41	66.11	21.2
8	13:54:30.142	1798.97	-10.21	-17.14	-10.49	0.04	1940.84	81.9	49.9	32.0	74.60	63.73	21.2
9	13:55:05.982	1727.44	-10.27	-16.82	-10.58	0.09	1867.34	81.9	49.9	32.1	71.79	61.34	21.3
10	13:55:41.822	1655.50	-10.34	-16.48	-10.70	0.07	1792.37	81.9	49.9	32.0	68.85	58.90	21.3
11	13:56:12.542	1593.51	-10.40	-16.18	-10.80	0.03	1727.36	81.9	49.9	32.0	66.28	56.78	21.4
12	13:56:43.262	1531.20	-10.47	-15.87	-10.90	0.00	1662.16	81.8	49.9	31.9	63.72	54.66	21.4
13	13:57:13.982	1468.56	-10.53	-15.55	-10.99	-0.02	1596.60	81.8	49.9	31.9	61.16	52.52	21.4
14	13:57:44.702	1405.57	-10.60	-15.21	-11.07	-0.01	1531.12	81.8	49.9	31.9	58.65	50.38	21.5
15	13:58:10.302	1352.82	-10.66	-14.92	-11.12	0.01	1476.32	81.9	49.9	32.0	56.57	48.58	21.5
16	13:58:35.902	1299.81	-10.72	-14.62	-11.18	0.00	1420.81	81.9	49.9	32.0	54.43	46.76	21.5
17	13:59:01.502	1246.55	-10.78	-14.31	-11.24	-0.04	1364.58	81.8	49.9	32.0	52.24	44.92	21.5
18	13:59:27.102	1193.02	-10.84	-13.98	-11.29	-0.08	1307.91	81.8	49.9	31.9	50.03	43.05	21.6
19	13:59:47.582	1150.00	-10.89	-13.71	-11.34	-0.11	1262.31	81.8	49.9	31.9	48.26	41.56	21.6
20	14:00:08.062	1106.80	-10.95	-13.43	-11.40	-0.16	1216.27	81.7	49.9	31.8	46.46	40.04	21.6
21	14:00:28.542	1063.41	-11.00	-13.15	-11.45	-0.23	1169.68	81.7	50.0	31.7	44.62	38.51	21.6
22	14:00:49.022	1019.84	-11.06	-12.85	-11.51	-0.28	1122.98	81.6	50.0	31.6	42.79	36.98	21.6
23	14:01:09.502	976.07	-11.12	-12.55	-11.57	-0.33	1076.19	81.6	50.0	31.6	40.97	35.44	21.7
24	14:01:29.982	932.10	-11.18	-12.23	-11.62	-0.37	1029.28	81.5	50.0	31.5	39.16	33.90	21.7
25	14:01:45.342	898.99	-11.22	-11.99	-11.66	-0.40	993.84	81.5	50.0	31.5	37.79	32.74	21.7
26	14:02:00.702	865.77	-11.27	-11.74	-11.71	-0.44	958.21	81.5	50.0	31.5	36.42	31.57	21.7
27	14:02:16.062	832.42	-11.32	-11.49	-11.75	-0.48	922.37	81.4	50.0	31.4	35.04	30.39	21.7
28	14:02:31.422	798.96	-11.36	-11.22	-11.79	-0.52	886.32	81.4	50.0	31.4	33.64	29.21	21.8
29	14:02:46.782	765.36	-11.41	-10.95	-11.84	-0.58	849.93	81.3	50.0	31.3	32.23	28.01	21.8
30	14:03:02.142	731.65	-11.46	-10.67	-11.89	-0.63	813.37	81.3	50.0	31.3	30.82	26.81	21.8
31	14:03:17.502	697.80	-11.52	-10.39	-11.93	-0.68	776.74	81.2	50.0	31.2	29.41	25.60	21.8
32	14:03:27.742	675.16	-11.55	-10.19	-11.96	-0.71	752.20	81.2	50.0	31.2	28.47	24.79	21.8
33	14:03:37.982	652.46	-11.59	-9.99	-11.99	-0.73	727.69	81.2	50.0	31.2	27.54	23.99	21.8
34	14:03:43.102	641.09	-11.61	-9.89	-12.00	-0.75	715.41	81.2	50.0	31.2	27.07	23.58	21.8
35	14:03:48.222	629.70	-11.62	-9.79	-12.02	-0.76	703.10	81.2	50.0	31.2	26.60	23.18	21.8
36	14:03:53.342	618.30	-11.64	-9.69	-12.03	-0.77	690.76	81.2	50.0	31.2	26.13	22.77	21.8
37	14:03:58.462	606.88	-11.66	-9.58	-12.05	-0.79	678.40	81.1	50.0	31.2	25.67	22.37	21.8
38	14:04:03.582	595.45	-11.68	-9.48	-12.06	-0.80	665.97	81.1	50.0	31.2	25.19	21.96	21.8
39	14:04:08.702	584.00	-11.70	-9.37	-12.08	-0.82	653.49	81.1	50.0	31.2	24.71	21.55	21.8
40	14:04:13.822	572.54	-11.72	-9.27	-12.09	-0.84	640.99	81.1	50.0	31.1	24.24	21.14	21.9
41	14:04:18.942	561.05	-11.74	-9.16	-12.11	-0.86	628.46	81.1	50.0	31.1	23.76	20.72	21.9
42	14:04:24.062	549.56	-11.75	-9.05	-12.12	-0.88	615.90	81.1	50.0	31.1	23.28	20.31	21.9
43	14:04:29.182	538.04	-11.77	-8.94	-12.13	-0.90	603.31	81.0	49.9	31.1	22.80	19.90	21.9
44	14:04:34.302	526.52	-11.79	-8.83	-12.15	-0.92	590.66	81.0	49.9	31.1	22.31	19.48	21.9

Table 2b. (Cont'd)

Photo number	GMT of frame exposure March 24, 1965	Spacecraft			Photograph (central reticle)						Scale, km		Deviation north, deg
		Altitude, km	Latitude, deg	Longitude, deg	Latitude, deg	Longitude, deg	Slant range, km	Incidence angle, deg	Phase angle, deg	Emission angle, deg	E-W	N-S	
45	14:04:39.422	514.97	-11.81	-8.71	-12.17	-0.94	577.99	81.0	50.0	31.1	21.83	19.06	21.9
46	14:04:44.542	503.41	-11.83	-8.60	-12.18	-0.97	565.28	81.0	50.0	31.0	21.34	18.64	21.9
47	14:04:49.662	491.83	-11.85	-8.49	-12.20	-0.99	552.54	81.0	50.0	31.0	20.85	18.22	21.9
48	14:04:54.782	480.23	-11.87	-8.37	-12.21	-1.01	539.78	80.9	50.0	31.0	20.37	17.80	21.9
49	14:04:59.902	468.62	-11.89	-8.25	-12.23	-1.04	526.98	80.9	50.0	31.0	19.88	17.38	21.9
50	14:05:05.022	456.99	-11.91	-8.13	-12.24	-1.06	514.14	80.9	50.0	30.9	19.39	16.96	21.9
51	14:05:10.142	445.34	-11.93	-8.01	-12.26	-1.09	501.27	80.9	50.0	30.9	18.89	16.53	21.9
52	14:05:15.262	433.68	-11.96	-7.89	-12.27	-1.12	488.37	80.8	50.0	30.9	18.40	16.11	21.9
53	14:05:20.382	422.00	-11.98	-7.77	-12.29	-1.14	475.44	80.8	50.0	30.8	17.91	15.68	21.9
54	14:05:25.502	410.30	-12.00	-7.64	-12.30	-1.17	462.48	80.8	50.0	30.8	17.41	15.26	22.0
55	14:05:30.622	398.58	-12.02	-7.52	-12.32	-1.20	449.49	80.8	50.0	30.8	16.92	14.83	22.0
56	14:05:35.742	386.85	-12.04	-7.39	-12.34	-1.23	436.46	80.7	50.0	30.8	16.42	14.40	22.0
57	14:05:40.862	375.09	-12.06	-7.26	-12.35	-1.26	423.39	80.7	50.0	30.7	15.92	13.97	22.0
58	14:05:45.982	363.32	-12.08	-7.13	-12.37	-1.29	410.30	80.7	50.0	30.7	15.42	13.54	22.0
59	14:05:51.102	351.53	-12.11	-7.00	-12.38	-1.32	397.17	80.6	50.0	30.6	14.92	13.10	22.0
60	14:05:56.222	339.73	-12.13	-6.87	-12.40	-1.35	384.01	80.6	50.0	30.6	14.42	12.67	22.0
61	14:06:01.342	327.90	-12.15	-6.73	-12.41	-1.38	370.83	80.6	50.0	30.6	13.92	12.24	22.0
62	14:06:06.462	316.06	-12.17	-6.60	-12.43	-1.41	357.63	80.6	50.0	30.5	13.42	11.80	22.0
63	14:06:11.582	304.19	-12.20	-6.46	-12.45	-1.44	344.39	80.5	50.0	30.5	12.92	11.36	22.0
64	14:06:16.702	292.31	-12.22	-6.32	-12.46	-1.47	331.12	80.5	50.0	30.5	12.42	10.93	22.0
65	14:06:21.822	280.41	-12.24	-6.18	-12.48	-1.50	317.81	80.5	50.0	30.5	11.91	10.49	22.0
66	14:06:26.942	268.49	-12.27	-6.04	-12.50	-1.53	304.47	80.4	50.0	30.4	11.41	10.05	22.0
67	14:06:32.062	256.55	-12.29	-5.89	-12.51	-1.56	291.09	80.4	50.0	30.4	10.90	9.61	22.0
68	14:06:37.182	244.59	-12.31	-5.75	-12.53	-1.59	277.69	80.4	50.0	30.4	10.40	9.16	22.0
69	14:06:42.302	232.61	-12.34	-5.60	-12.54	-1.63	264.24	80.3	50.0	30.3	9.89	8.72	22.0
70	14:06:47.422	220.61	-12.36	-5.45	-12.56	-1.66	250.76	80.3	50.0	30.3	9.38	8.28	22.1
71	14:06:52.542	208.59	-12.39	-5.30	-12.57	-1.69	237.24	80.3	50.0	30.3	8.87	7.83	22.1
72	14:06:57.662	196.55	-12.41	-5.14	-12.59	-1.73	223.68	80.3	50.0	30.2	8.36	7.38	22.1
73	14:07:02.782	184.48	-12.44	-4.99	-12.61	-1.76	210.09	80.2	50.0	30.2	7.85	6.93	22.1
74	14:07:07.902	172.40	-12.46	-4.83	-12.62	-1.80	196.45	80.2	50.0	30.2	7.34	6.48	22.1
75	14:07:13.022	160.30	-12.49	-4.67	-12.64	-1.83	182.78	80.1	50.0	30.1	6.82	6.03	22.1
76	14:07:18.142	148.18	-12.51	-4.51	-12.65	-1.87	169.06	80.1	50.0	30.1	6.31	5.58	22.1
77	14:07:23.262	136.03	-12.54	-4.35	-12.67	-1.91	155.31	80.1	50.0	30.1	5.79	5.13	22.1
78	14:07:28.382	123.87	-12.56	-4.18	-12.68	-1.95	141.51	80.0	50.0	30.0	5.28	4.67	22.1
79	14:07:33.502	111.68	-12.59	-4.01	-12.70	-1.99	127.67	80.0	50.0	30.0	4.76	4.21	22.1
80	14:07:38.622	99.47	-12.62	-3.84	-12.72	-2.03	113.79	80.0	50.0	29.9	4.24	3.76	22.1
81	14:07:43.742	87.24	-12.64	-3.67	-12.73	-2.07	99.86	79.9	50.1	29.9	3.72	3.30	22.1
82	14:07:48.862	74.99	-12.67	-3.49	-12.75	-2.11	85.89	79.9	50.1	29.9	3.20	2.84	22.1
83	14:07:53.982	62.71	-12.70	-3.31	-12.76	-2.15	71.88	79.9	50.1	29.8	2.67	2.37	22.1
84	14:07:59.102	50.42	-12.73	-3.13	-12.78	-2.19	57.82	79.8	50.1	29.8	2.15	1.91	22.1
85	14:08:04.222	38.10	-12.75	-2.95	-12.79	-2.23	43.73	79.8	50.1	29.7	1.63	1.44	22.1
86	14:08:09.342	25.75	-12.78	-2.77	-12.81	-2.28	29.58	79.7	50.0	29.7	1.10	0.98	22.1
87	14:08:14.462	13.39	-12.81	-2.58	-12.82	-2.32	15.39	79.7	50.0	29.7	0.57	0.51	22.1
88	14:08:19.582	1.00	-12.84	-2.39	-12.84	-2.37	1.15	79.6	50.0	29.6	0.04	0.04	22.2
IMPACT	14:08:19.994												

Table 2. (Cont'd)
c. Camera P₁

Photo number	GMT of frame exposure March 24, 1965	Spacecraft			Photograph (central reticle)						Scale, km		Deviation north, deg
		Altitude, km	Latitude, deg	Longitude, deg	Latitude, deg	Longitude, deg	Slant range, km	Incidence angle, deg	Phase angle, deg	Emission angle, deg	E-W	N-S	
1	14:08:10.306	23.43	-12.79	-2.73	-12.85	-2.36	25.89	79.6	54.6	25.4	0.78	0.68	24.9
2	14:08:11.146	21.40	-12.79	-2.70	-12.85	-2.37	23.65	79.6	54.6	25.4	0.71	0.62	24.9
3	14:08:11.986	19.37	-12.80	-2.67	-12.85	-2.37	21.41	79.6	54.6	25.4	0.64	0.56	24.9
4	14:08:12.826	17.34	-12.80	-2.64	-12.85	-2.37	19.17	79.6	54.6	25.4	0.58	0.50	24.9
5	14:08:13.666	15.31	-12.81	-2.61	-12.84	-2.37	16.93	79.6	54.6	25.4	0.51	0.45	24.9
6	14:08:14.506	13.28	-12.81	-2.58	-12.84	-2.37	14.69	79.6	54.6	25.4	0.44	0.39	24.9
7	14:08:15.346	11.25	-12.81	-2.54	-12.84	-2.37	12.44	79.6	54.6	25.4	0.37	0.33	25.0
8	14:08:16.186	9.22	-12.82	-2.51	-12.84	-2.37	10.20	79.6	54.6	25.4	0.31	0.27	25.0
9	14:08:17.026	7.19	-12.82	-2.48	-12.84	-2.37	7.95	79.6	54.6	25.4	0.24	0.21	25.0
10	14:08:17.866	5.15	-12.83	-2.45	-12.84	-2.37	5.70	79.6	54.6	25.4	0.17	0.15	25.0
11	14:08:18.706	3.12	-12.83	-2.42	-12.84	-2.37	3.45	79.6	54.6	25.4	0.10	0.09	25.0
12	14:08:19.546	1.08	-12.84	-2.39	-12.84	-2.37	1.20	79.6	54.6	25.4	0.04	0.03	25.0
IMPACT	14:08:19.994												

Table 2. (Cont'd)
d. Camera P₂

Photo number	GMT of frame exposure March 24, 1965	Spacecraft			Photograph (central reticle)						Scale, km		Deviation north, deg
		Altitude, km	Latitude, deg	Longitude, deg	Latitude, deg	Longitude, deg	Slant range, km	Incidence angle, deg	Phase angle, deg	Emission angle, deg	E-W	N-S	
1	14:08:10.706	22.46	-12.79	-2.72	-12.83	-2.37	24.71	79.6	55.0	24.8	0.74	0.71	24.3
2	14:08:11.546	20.43	-12.79	-2.68	-12.83	-2.37	22.48	79.6	55.0	24.8	0.68	0.64	24.3
3	14:08:12.386	18.40	-12.80	-2.65	-12.83	-2.37	20.25	79.6	55.0	24.8	0.61	0.58	24.3
4	14:08:13.226	16.37	-12.80	-2.62	-12.83	-2.37	18.02	79.6	55.0	24.8	0.54	0.52	24.3
5	14:08:14.066	14.34	-12.81	-2.59	-12.83	-2.37	15.79	79.6	55.0	24.8	0.48	0.45	24.3
6	14:08:14.906	12.31	-12.81	-2.56	-12.84	-2.37	13.56	79.6	55.0	24.8	0.41	0.39	24.3
7	14:08:15.746	10.28	-12.82	-2.53	-12.84	-2.37	11.32	79.6	55.0	24.8	0.34	0.32	24.3
8	14:08:16.586	8.25	-12.82	-2.50	-12.84	-2.37	9.09	79.6	55.0	24.8	0.27	0.26	24.3
9	14:08:17.426	6.22	-12.83	-2.47	-12.84	-2.37	6.85	79.6	55.0	24.8	0.21	0.20	24.3
10	14:08:18.266	4.18	-12.83	-2.44	-12.84	-2.37	4.61	79.6	55.0	24.8	0.14	0.13	24.3
11	14:08:19.106	2.15	-12.84	-2.40	-12.84	-2.37	2.37	79.6	55.0	24.8	0.07	0.07	24.3
IMPACT	14:08:19.994												

Table 2. (Cont'd)
e. Camera P₃

Photo number	GMT of frame exposure March 24, 1965	Spacecraft			Photograph (central reticle)						Scale, km		Deviation north, deg
		Altitude, km	Latitude, deg	Longitude, deg	Latitude, deg	Longitude, deg	Slant range, km	Incidence angle, deg	Phase angle, deg	Emission angle, deg	E-W	N-S	
1	14:08:10.506	22.94	-12.79	-2.72	-12.84	-2.35	25.56	79.7	53.6	26.4	2.19	2.07	23.3
2	14:08:11.346	20.92	-12.79	-2.69	-12.84	-2.35	23.31	79.7	53.6	26.4	2.00	1.89	23.3
3	14:08:12.186	18.89	-12.80	-2.66	-12.84	-2.35	21.05	79.7	53.6	26.4	1.81	1.70	23.3
4	14:08:13.026	16.86	-12.80	-2.63	-12.84	-2.35	18.79	79.7	53.6	26.4	1.61	1.52	23.3
5	14:08:13.866	14.83	-12.81	-2.60	-12.84	-2.36	16.53	79.7	53.6	26.4	1.42	1.34	23.3
6	14:08:14.706	12.80	-12.81	-2.57	-12.84	-2.36	14.27	79.7	53.6	26.4	1.22	1.16	23.3
7	14:08:15.546	10.77	-12.82	-2.54	-12.84	-2.36	12.01	79.6	53.6	26.4	1.03	0.97	23.3
8	14:08:16.386	8.73	-12.82	-2.51	-12.84	-2.36	9.74	79.6	53.6	26.4	0.84	0.79	23.3
9	14:08:17.226	6.70	-12.83	-2.47	-12.84	-2.36	7.48	79.6	53.6	26.4	0.64	0.61	23.3
10	14:08:18.066	4.67	-12.83	-2.44	-12.84	-2.37	5.21	79.6	53.6	26.4	0.45	0.42	23.3
11	14:08:18.906	2.63	-12.83	-2.41	-12.84	-2.37	2.94	79.6	53.6	26.4	0.25	0.24	23.3
12	14:08:19.746	0.60	-12.84	-2.38	-12.84	-2.37	0.67	79.6	53.6	26.4	0.06	0.05	23.3
IMPACT	14:08:19.994												

Table 2. (Cont'd)
f. Camera P₄

Photo number	GMT of frame exposure March 24, 1965	Spacecraft			Photograph (central reticle)						Scale, km		Deviation north, deg
		Altitude, km	Latitude, deg	Longitude, deg	Latitude, deg	Longitude, deg	Slant range, km	Incidence angle, deg	Phase angle, deg	Emission angle, deg	E-W	N-S	
1	14:08:10.906	21.98	-12.79	-2.71	-12.83	-2.35	24.39	79.7	53.9	25.9	2.14	2.00	23.0
2	14:08:11.746	19.95	-12.79	-2.68	-12.83	-2.36	22.14	79.7	53.9	25.9	1.94	1.82	23.0
3	14:08:12.586	17.92	-12.80	-2.65	-12.83	-2.36	19.89	79.7	53.9	25.9	1.74	1.63	23.0
4	14:08:13.426	15.89	-12.80	-2.62	-12.83	-2.36	17.64	79.6	53.9	25.9	1.55	1.45	23.0
5	14:08:14.266	13.86	-12.81	-2.58	-12.83	-2.36	15.39	79.6	53.9	25.9	1.35	1.26	23.0
6	14:08:15.106	11.83	-12.81	-2.55	-12.83	-2.36	13.14	79.6	53.9	25.9	1.15	1.08	23.0
7	14:08:15.966	9.75	-12.82	-2.52	-12.83	-2.36	10.83	79.6	53.9	25.9	0.95	0.89	23.0
8	14:08:16.786	7.77	-12.82	-2.49	-12.84	-2.36	8.63	79.6	53.9	25.9	0.76	0.71	23.0
9	14:08:17.626	5.73	-12.83	-2.46	-12.84	-2.37	6.37	79.6	53.9	25.9	0.56	0.52	23.0
10	14:08:18.466	3.70	-12.83	-2.43	-12.84	-2.37	4.11	79.6	53.9	25.9	0.36	0.34	23.0
11	14:08:19.306	1.67	-12.84	-2.40	-12.84	-2.37	1.85	79.6	53.9	25.9	0.16	0.15	23.0
IMPACT	14:08:19.994												

REFERENCES

1. Rindfleisch, T. C., and Willingham, D. E., *Figure of Merit as a Measure of Picture Resolution*, Technical Report No. 32-666, Jet Propulsion Laboratory, Pasadena, California, September 1, 1965.
2. Kirhofer, W. E., *Television Constraints and Digital Computer Program*, Technical Report No. 32-667, Jet Propulsion Laboratory, Pasadena, California (to be published).
3. Sytinskaya, N. N., and Sharonov, V. V., "Study of the Reflecting Power of the Moon's Surface," *Uchenye Zapiski Lgu*, No. 153 (1952), p. 114. (Translated by Space Technology Laboratories, Inc., Los Angeles, California, as STL-TR-61-5110-23, May 1961.)
4. Willingham, D. E., *The Lunar Reflectivity Model for Ranger Block III Analysis*, Technical Report No. 32-664, Jet Propulsion Laboratory, Pasadena, California, November 2, 1964.
5. Smith, G. M., and Willingham, D. E., *Ranger Photometric Calibration*, Technical Report No. 32-665, Jet Propulsion Laboratory, Pasadena, California, August 15, 1965.

